Sensors and Materials, Vol. 38, No. 8 (2026) 4637–4654
MYU Tokyo

S & M 4586

Sensor-based Knowledge Graph Modeling of Cognitive Pathways in Brand Information Recognition

Li Liu,[1*] Zhi Wang,[2] and Xiaodan Zhang[2]

[1]Research Center for Hubei Brand Development, Wenhua College, Wuhan 430000, China
[2]Faculty of Information Science and Technology, Wenhua College, Wuhan 430000, China

(Received May 11, 2026; accepted August 19, 2026)

Keywords: knowledge graph, Neo4j, automated scoring algorithms, information overload, data veracity, misleading information

The evaluation of consumer visual attention often relies on static area-of-interest (AOI) metrics or self-reports, which fail to capture continuous cognitive pathways. To address this limitation, high-frequency eye-tracking sensors are integrated with knowledge graph modeling to analyze dynamic brand recognition. Ocular data from 60 participants were recorded using the SensoMotoric Instruments Remote Eye Directorate (250 Hz sampling rate, 0.03° precision) during simulated e-commerce browsing. Raw gaze coordinates and pupil metrics were compressed into AOI sequences and modeled as a directed weighted graph. Weighted degree centrality identified price information (a 485.6 s fixation), main product images (450.2 s), and the reviews of first-time consumers in the digital marketing environment (users, 398.1 s) as the primary anchors of attention. Graph extraction results showed a dominant overview-to-valuation pathway (brand logo → main image → product title → price). New users showed higher path complexity (mean = 1.85, standard deviation = 0.42) than experienced users (mean = 1.31, standard deviation = 0.35), whereas impulsive users concentrated on promotional cues. Pupil dilation correlated with path complexity ($r = 0.58$, $p < 0.01$), confirming its role as a cognitive load indicator. The framework developed in this study advances sensor-based cognitive modeling and supports neuromorphic vision sensing and human–computer interaction. Limitations include reliance on desktop-mounted sensors and static layouts; future work must extend to mobile and adaptive interfaces.

1. Introduction

The proliferation of digital media has resulted in significant information overload for consumers. In an overwhelming amount of information, it is challenging to determine how brands effectively convey their values and capture consumer attention in a competitive market. To assess the brand recognition level among digital marketing consumers (users) and its effectiveness in raising recognition, questionnaires and focus group interviews have been widely adopted. However, the results vary according to subjective memories and self-reporting of

*Corresponding author: e-mail: liuli1@whc.edu.cn
https://doi.org/10.18494/SAM6421

ISSN 0914-4935
https://myukk.org/

respondents and interviewees, and are prone to bias and fail to capture the instantaneous, subconscious consumer's cognitive processes of recognizing brands. To address such limitations in assessing the brand recognition levels and paths of consumers, more objective, data-driven methods are necessary. Such methods should also be capable of providing data to understand consumer behavior in real-time. Therefore, sensor technology, especially eye-tracking sensors, has been introduced to objectively quantify human visual attention and cognitive mechanisms.

Recent advances in materials and integrated systems have significantly improved the precision of eye movement tracking.[1] Linear array sensors,[2] carbon-nanotube-paper-composite capacitive sensors,[3] and flexible piezoelectric sensors[4] enable the continuous and safe monitoring of oculomotor movements. These high-frequency sensors are widely used in medical diagnostics,[5,6] non-technical skill assessment,[7] and the automated assessment of emotional responses for packaging labeling.[8] By employing a high-frequency eye-tracking sensor, one can collect the granular data required to study brand recognition.

Despite advances in eye-tracking technology, challenges remain in applying these sensors effectively to brand recognition research. Most studies rely on static area-of-interest (AOI) metrics such as first fixation time or total gaze duration, which overlook dynamic visual transitions and continuous cognitive pathways. As a result, the exploration process is only partially understood. Algorithmic development adds further complexity: automated scoring methods have been used in three-dimensional environments, but they lack the topological depth needed to capture how consumers acquire information through transitions across complex modules. Traditional AOI measures[9] and probabilistic models such as Markov chains[10] are used to capture isolated or sequential behaviors but fail to represent systemic pathways. Sensor-graph approaches have been applied to spatial navigation, but only in a few studies are high-frequency physiological signals integrated with knowledge graph (KG) architectures to track cognitive load in brand recognition. To address these limitations, we adopted a sensor-integrated KG and high-frequency oculomotor data (250 Hz tracking, microsaccade detection) with graph-theoretic modeling to map continuous pathways, quantify search behavior, and measure cognitive workload through pupil dilation.

By structuring gaze data into interconnected nodes and edges, the developed framework enables the identification of patterns in brand recognition that static measures cannot capture. Physiological indicators such as pupil diameter and scanning amplitude are fused with KG models to quantify workload[11] and path complexity. This fusion enhances the responsiveness of eye-tracking systems and extends applications to emotion recognition[12] and fatigue assessment.[13] The framework supports sensor-integrated human–computer interaction[3] and neuromorphic vision sensing,[14] advancing personalized and adaptive digital marketing environments.

2. Methods

We constructed a dynamic map of brand information recognition by extending static eye-tracking metrics into a continuous behavioral framework. The approach captured the full trajectory of consumer visual exploration, addressing limitations of subjective reporting and isolated AOI indicators. Experiments were conducted to determine whether high-frequency cognitive pathways emerge across brand recognition tasks: sequences such as brand logo → main image → price. The analysis results were compared in terms of pathway structures between new and experienced users to examine how decision-making styles, such as impulsive versus rational approaches, influenced attention shifts toward promotional or technical information. These results enable the understanding of consumer cognitive processes and advance sensor-based methodologies for brand recognition analysis.

To model structural dependencies, gaze and pupil data were organized into a knowledge graph, where nodes represent information entities and edges represent visual transitions. Graph features were evaluated using automated scoring algorithms that rank items quantitatively on the basis of relevance and quality metrics. Implementation was carried out in the Neo4j database, a graph database optimized for storing and querying highly interconnected networks, ensuring efficient handling of complex cognitive pathways.

2.1 Experiment

2.1.1 Measurement

For high-precision oculomotor monitoring, we employed the SensoMotoric Instruments Remote Eye Directorate 250 (250 Hz sampling rate, 0.03° precision) (SMI RED250) mobile desktop eye tracker (SensoMotoric Instruments, Germany) (Table 1). This high-frequency sensor captures granular data required for mapping complex visual transitions. The device integrates an optoelectronic assembly consisting of high-power infrared (IR) light-emitting diodes (LEDs, λ = 850 nm) and a high-frame-rate monochrome CMOS image sensor operating at 250 Hz. The IR LED array projects invisible near-infrared illumination onto the ocular surface, producing bright-pupil and corneal reflection signals. The CMOS sensor records 250 frames per second with a spatial precision of the root mean square (*RMS*) of 0.03°.[15,16]

The SMI RED250 eye tracker was calibrated, which was controlled by SMI iView X software using a standard nine-point grid routine. The calibration points were presented sequentially as animated red targets (a visual angle of 0.5°) systematically distributed across the 3200 × 1920

Table 1
Specifications of SMI RED250.

Parameter	Value	Description
Sampling rate	250 Hz	250 eye movement data points sampled per second
Accuracy	0.4°	Average angular error under ideal conditions
Precision	0.03° (root-mean-square deviation between successive samples)	Root-mean-square deviation between successive samples
Head movement range	40 × 20 cm^2	Permissible head motion area at a viewing distance of 60 cm
Calibration method	9-point calibration	Covers major screen regions to ensure full-screen accuracy
Data output	Gaze coordinates, pupil diameter, and timestamps	Raw data stream

pixel stimulus screen: four at the screen corners (10% margin from screen edges), four at the midpoints of the screen edges, and one at the screen center.(17,18) The participants were instructed to fixate on each target point as it appeared. Spatial accuracy was validated immediately following calibration, and the routine was repeated if the mean angular error exceeded 0.5° for both eyes.(19)

Using the data, we calculated weighted degree centrality [$C_w(v)$] to quantify the importance of each AOI in the cognitive path graph. It is defined as

$$C_w(v) = \sum_{u \in In(v)} w(u \to v) + \sum_{u \in Out(v)} w(v \to u). \tag{1}$$

Here, v is the node representing AOI, $In(v)$ is the set of nodes with edges pointing into v, $Out(v)$ is the set of nodes with edges starting from v, $w(u \to v)$ is the weight of the edge from node u to node v, defined as the transition frequency between AOIs, and $w(u \to v)$ is the transition frequency from AOI u to AOI v. This measure reflects the attraction of attention to a node and its connectivity within the browsing network.(20,21) Path complexity is calculated to understand the structural characteristics of a user's browsing sequence. It is calculated as

$$Path\,complexity = \frac{L}{U}. \tag{2}$$

Here, L is the total path length (number of transitions in a sequence), and U is the number of visited AOIs. Higher values indicate exploratory or repetitive browsing, and lower values reflect direct, goal-oriented navigation.(14,22) *Cognitive load* (*CL*) is calculated using changes in pupil diameter, a physiological indicator of mental effort. The relative change in pupil diameter is computed as

$$\mathrm{C}L = \frac{\overline{PD}_{task} - \overline{PD}_{baseline}}{\overline{PD}_{baseline}}. \tag{3}$$

Here, $\overline{PD}_{task}$ is the average pupil diameter during task execution and $\overline{PD}_{baseline}$ is the baseline diameter measured during calibration. Increases in *CL* indicate higher cognitive workload.(11)

RED250's high sampling rate (250 Hz) and precision (*RMS* of 0.03°) ensured the accurate detection of microsaccades, fixation durations, and subtle pupil diameter changes. By combining graph-theoretic measures (weighted degree centrality and path complexity) with physiological indicators (pupil diameter change), we selected the methods to link sensor-captured oculomotor data to cognitive processes. This integration advances sensor-based cognitive modeling and supports applications in human–computer interaction,(23) neuromorphic vision sensing,(14) and emotion recognition systems.(12)

2.1.2 Simulation

To simulate a digital marketing environment, we designed a product detail page for a virtual brand, NovaTech (Fig. 1). The layout consisted of ten distinct information modules (3200 × 1920 pixels), arranged to encourage natural scrolling behavior and to reflect the structure of a typical e-commerce interface. Each module represented an element of consumer decision-making: the brand logo (A1) and main product image (A2) provided immediate brand identity and visual appeal; the product title (A3) and user ratings (A4) conveyed essential descriptive and evaluative

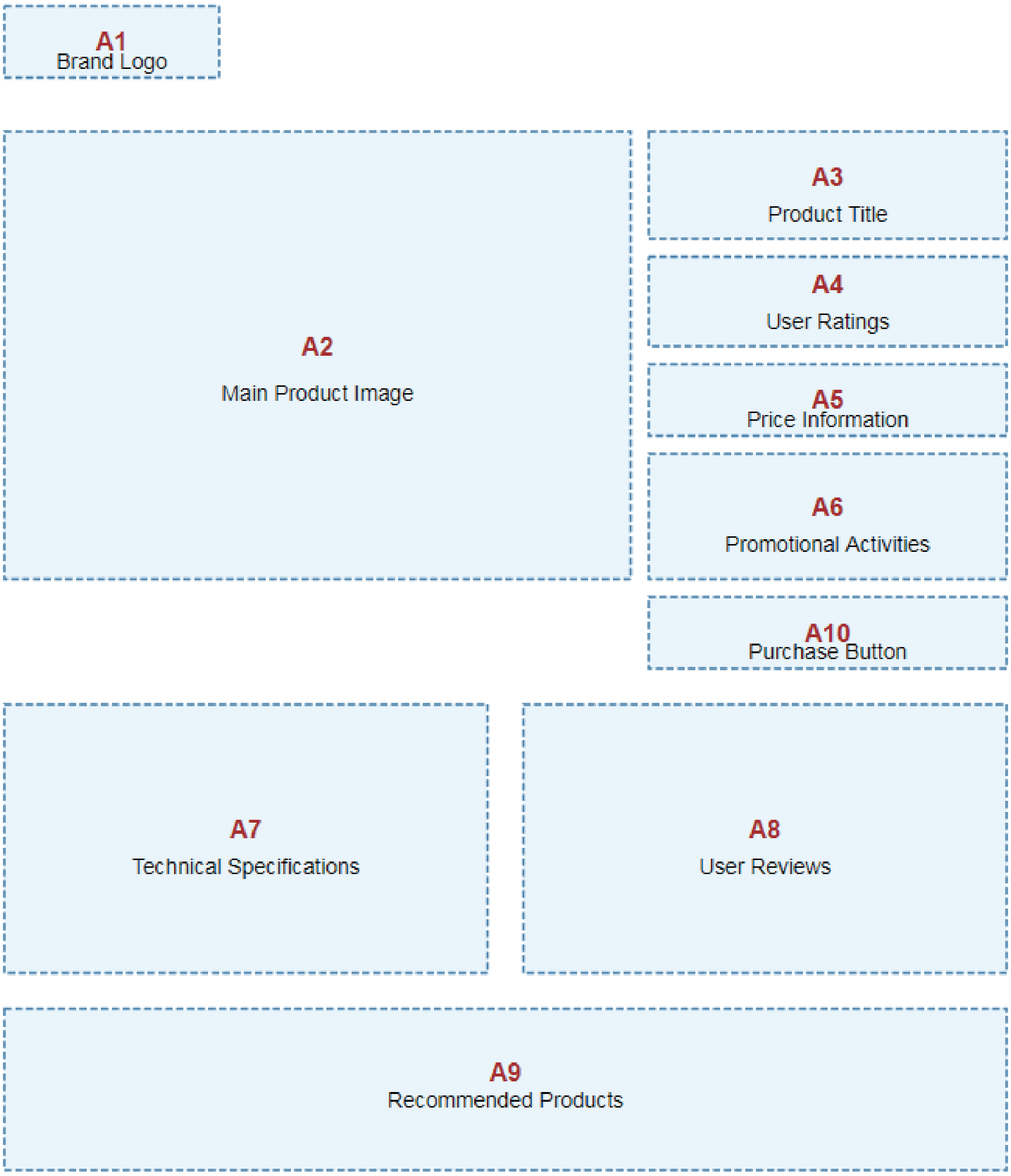

Fig. 1. (Color online) Layout of NovaTech product detail webpage, showing 10 AOIs (A1–A10) to simulate digital marketing environment.

information; price information (A5) and promotional activities (A6) highlighted economic considerations; technical specifications (A7) and user reviews (A8) offered detailed product knowledge and social proof; recommended products (A9) simulated cross-selling strategies; and the purchase button (A10) represented the final conversion point. This structured arrangement was used to systematically examine how consumers transition between modules and capture cognitive pathways in brand information recognition (Table 2).

The experimental procedure followed a five-step standardized protocol to ensure data validity (Fig. 2).

- Preparation: Signing of informed consent and completion of the consumer style inventory (CSI) questionnaire
- Calibration: A 9-point calibration was performed. Accuracy was maintained below 0.5° of error.
- Stimulus presentation: A 3-s fixation cross preceded the free-browsing task.
- Synchronous recording: The sensor recorded gaze coordinates, timestamps, and pupil diameter, the latter serving as an index for cognitive workload.[11]
- Post-interview: Qualitative data on decision-making were collected to supplement sensor data.

In the experiment, we recruited 60 participants through university mailing lists, online bulletin boards, and local community advertisements. The sample included 32 males and 28

Table 2
Definition of AOIs in simulation.

Code	AOI	Description
A1	Brand logo	Brand identifier located at the top of the page
A2	Main product image	Large-scale image showcasing the product's appearance
A3	Product title	Text containing brand name, model, and core selling points
A4	User ratings	Star-based rating score and total number of ratings
A5	Price information	Current price, original price, discount information, etc.
A6	Promotional activities	Coupons, minimum-purchase discounts, gifts, etc.
A7	Technical specifications	Detailed list of product parameters
A8	User reviews	Purchase reviews and user-submitted photos from other customers
A9	Recommended products	Algorithmically suggested related or alternative products
A10	Purchase button	"Add to Cart" or "Buy Now" button

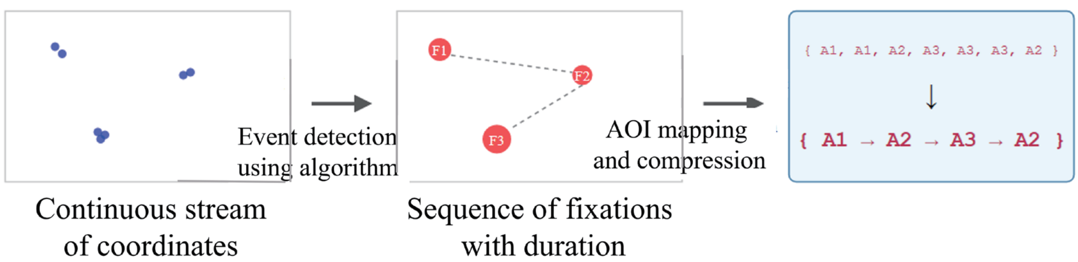

(a) (b) (c)

Fig. 2. (Color online) Transformation process from eye-tracking data to cognitive path sequence: (a) Raw gaze points, (b) fixation sequence, and (c) cognitive path sequence.

females, with a mean age of 22.7 years [standard deviation (*SD*) = 2.5]. All participants had normal or corrected vision (Table 3). On the basis of the preliminary questionnaire and CSI analysis, participants were classified as either new or experienced users. Classification was determined by category experience and online shopping frequency. Because NovaTech was introduced as a virtual brand to control for brand equity bias, experienced users were defined as consumers highly familiar with e-commerce layouts and electronics shopping workflows, reporting at least three transactions per month. New users were defined as novice online shoppers unfamiliar with structured e-commerce layouts, reporting fewer than one transaction per month.

In addition to age and gender, the participants provided information on educational background, socioeconomic status, and online shopping experience. Most were undergraduate or graduate students (78%), while the remainder were employed in entry-level professional positions. Household income levels ranged from low to middle socioeconomic brackets, reflecting typical young adult demographics. These background traits were documented because education, income, and occupational status can affect decision-making strategies, risk tolerance, and familiarity with digital marketing environments.

To ensure participant grouping, we conducted surveys using a preliminary questionnaire survey and CSI.[24] The preliminary questionnaire survey was conducted to evaluate platform familiarity and e-commerce purchasing frequency to categorize participants into new versus experienced users. CSI was used to evaluate cognitive decision-making orientation to differentiate impulsive from rational users.

The preliminary questionnaire was designed using established usability engineering and user-profiling methodologies to assess participants' online shopping habits, familiarity with e-commerce platforms, and domain expertise. Its creation and validation followed four structured steps (Table 4).[25,26] First, constructs were selected to distinguish novice from experienced online shoppers. Two dimensions were prioritized: purchasing frequency, measured as the number of transactions per month, and familiarity with standard e-commerce page layouts, including product images, specification tabs, and review modules. Second, survey items and scales were formulated to capture these constructs. Purchasing frequency was measured using continuous numerical metrics, while layout familiarity was assessed with a five-point Likert scale (1 = strongly disagree, 5 = strongly agree). This design enabled both behavioral and

Table 3
Demographics of participants in experiment.

Variable	Category	*N*	%
Gender	Male	32	53.3
	Female	28	46.7
Age (years old)	18–22	35	58.3
	23–28	25	41.7
User type	New user	30	50.0
	Experienced user	30	50.0
Decision-making style	Impulsive	28	46.7
	Rational	32	53.3

Table 4
Items of preliminary questionnaire.

Item No.	Construct/dimension	Question
Q1	Gender	"What is your gender?"
Q2	Age	"What is your age in years?"
Q3	Visual status	"Select your visual condition:"
Q4	Shopping frequency	"How frequently do you make online purchases on e-commerce platforms such as Amazon, Taobao, and Coupang?"
Q5	Category experience	"Have you previously purchased consumer electronics or smart devices online?"
Q6	Layout familiarity	"I am familiar with standard product detail page layouts on e-commerce websites such as the location of main product images, technical specification tables, price blocks, and customer review sections."

perceptual profiling. Third, expert review refined the questionnaire. Three specialists in human–computer interaction, e-commerce UX design, and consumer psychology evaluated the draft to ensure clarity, content validity, and domain relevance. They eliminated semantic ambiguity, verified that layout familiarity constructs reflected modern interface architectures, and confirmed the appropriateness of quantitative thresholds for user segmentation. Finally, thresholds were defined to classify participants systematically. Experienced users were identified as those reporting three or more purchases per month and a layout familiarity score of at least 4.0. New users were defined as those reporting fewer than one purchase per month and a layout familiarity score of 2.0 or lower. These thresholds provided clear segmentation for subsequent analysis.

CSI was revised from the established eight-dimension decision-style framework to isolate impulsive versus rational decision-making characteristics (Table 5).(24) The participants completed a preliminary questionnaire and an adapted CSI before the eye-tracking experiment.(24)

2.2 Data processing and modeling

2.2.1 Data processing

In the experiment, raw data were obtained using the high-frequency eye-tracking sensor and supplementary questionnaire surveys. The raw data collected include the following.

- Gaze coordinates: The precise screen locations of the user's eye movements, recorded at a high sampling frequency of 250 Hz.
- Timestamps: Temporal data for every sampled point for the calculation of gaze duration and sequence of visual attention
- Pupil diameter: Continuous measurement of the participant's pupil size, which serves as a physiological indicator of cognitive load and emotional arousal
- Demographic and psychographic data: Information regarding participant age, gender, and consumption styles (impulsive or rational) obtained through preliminary surveys and CSI
- Post-task feedback: The participants' decision-making styles and browsing experience.

Table 5
Items of CSI questionnaires.

Subscale	Item No.	Statement
Impulsive style	CSI-1	"I often make spontaneous purchases without planning."
	CSI-2	"Promotional discounts, coupons, and flash sales immediately draw my attention."
	CSI-3	"When I see an attractive deal on a product page, I tend to buy it right away without checking other details."
	CSI-4	"I spend little time evaluating technical parameters if the product appearance or price looks appealing."
Rational/perfectionistic style	CSI-5	"I carefully read technical specifications and product parameter tables before making a purchase."
	CSI-6	"Customer ratings, detailed user reviews, and buyer photos are essential factors in my buying decisions."
	CSI-7	"I systematically compare multiple product attributes such as price vs specification vs user feedback to ensure I choose the best option."
	CSI-8	"I spend considerable time verifying information to minimize the risk of making a wrong purchasing decision."

The data were synchronously recorded using the SMI BeGaze and iView X software packages to ensure alignment between the visual stimulus and the physiological responses. Raw data obtained were processed using an event detection algorithm (SMI BeGaze). Eye fixations were defined by a velocity threshold of lower than 30 °/s and a gaze duration of longer than 80 ms, whereas saccades were identified by velocities of higher than 30 °/s. The data were also used for the calculation of capture speed (time to first fixation) and processing depth (total gaze duration) (Table 6).

2.2.2 Cognitive path sequence

To transform raw sensor data into a structured cognitive pathway, we mapped fixation sequences to discrete AOIs (Fig. 2).

1. Event detection: Each fixation point coordinate was assigned to its corresponding AOI code.
2. AOI mapping and compression: Consecutive fixations within the same AOI were merged to represent macrolevel transitions. For example, the sequence {A1, A1, A2, A3, A3} was compressed into {A1, A2, A3}.

The data were modeled as a weighted directed graph, $G = (V, E)$. The nodes (V) represent AOIs, each annotated with attributes such as total gaze duration, fixation count, and average pupil diameter to capture physiological responses. The edges (E) represent visual transitions ($u \to v$), characterized by transition frequency and average saccade amplitude. To quantify the likelihood of transitions, the transition probability $P(v|u)$ was defined as

$$P(v \mid u) = \frac{Count(u \to v)}{\sum_{w \in Out(u)} Count(u \to w)} . \tag{4}$$

Table 6
Eye-tracking metrics and their definitions used in this study.

Metric	Definition	Implication
Time to first fixation	Time elapsed from stimulus onset to the first fixation on a given AOI	Visual salience and speed of attentional capture
Total gaze duration	Sum of all gaze durations within given AOI	Depth of information processing and level of interest
Fixation count	Total number of fixations within given AOI	Degree of attention allocation and frequency of re-examination
Average pupil diameter	Mean pupil diameter during fixation on given AOI	Index of cognitive load and emotional arousal
Saccade amplitude	Angular distance between two successive fixation points	Breadth of visual search and scope of information scanning

Here, $Count(u \rightarrow v)$ is the number of times participants' eye movements (saccades) transitioned from AOI u to AOI v. This is the raw frequency of that specific transition. $\sum_{w \in Out(u)} Count(u \rightarrow w)$ represents the denominator, which sums all transition counts from node u to any other AOI w in its outgoing set. It is the total number of transitions that start at AOI u, regardless of where they end. $Out(u)$ is the set of all AOIs that can be reached directly from AOI u. This defines the possible destinations of a gaze shift starting at u. This equation was used to normalize transition counts by the total outgoing transitions from node u, capturing the relative probability of moving from one AOI to another. The resulting dataset, collected from 60 participants, was imported into the Neo4j graph database for the construction of a robust analytical framework for identifying high-frequency cognitive pathway patterns across different user demographics, as illustrated in Fig. 3.

4. Results and Discussion

4.1 Cognitive path patterns

4.1.1 Information nodes and sensor-based attention mapping

To identify influential information nodes (AOIs), we analyzed the weighted degree centrality and total gaze duration derived from high-frequency eye-tracking sensor data. The sensors integrated with capacitive and piezoelectric modules captured microlevel ocular movements with high temporal precision, enabling the accurate quantification of gaze behavior.[23] The weighted degree centrality metric, defined as the sum of incoming and outgoing edge weights, reflects the role of each AOI in the information flow network. As shown in Table 7 and Fig. 4, AOIs corresponding to price information (A5), main product image (A2), and user reviews (A8) exhibited the highest fixation durations and normalized centrality values. These nodes serve as cognitive anchors in the decision-making process. The high centrality of A1 (brand logo), despite its moderate fixation duration, suggests its function as an initial orientation point, which is consistent with prior sensor-based studies on visual branding attention.[27] The strong correlation between gaze duration and weighted degree centrality is observed in Fig. 4, confirming that

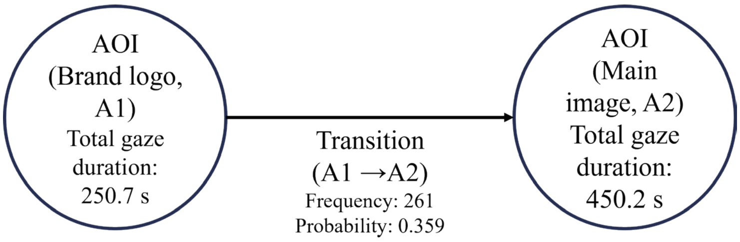

Fig. 3. Example of cognitive path KG model.

Table 7
Results of key node analysis.

Code	AOI	Total gaze duration (s)	Normalized weighted centrality
A5	Price information	485.6	1.00
A2	Main product image	450.2	0.92
A8	User reviews	398.1	0.85
A7	Technical specifications	355.9	0.78
A3	Product title	288.4	0.71
A1	Brand logo	250.7	0.65
A6	Promotional activities	210.3	0.59
A10	Purchase button	155.2	0.43
A4	User ratings	120.5	0.38
A9	Recommended products	88.9	0.25

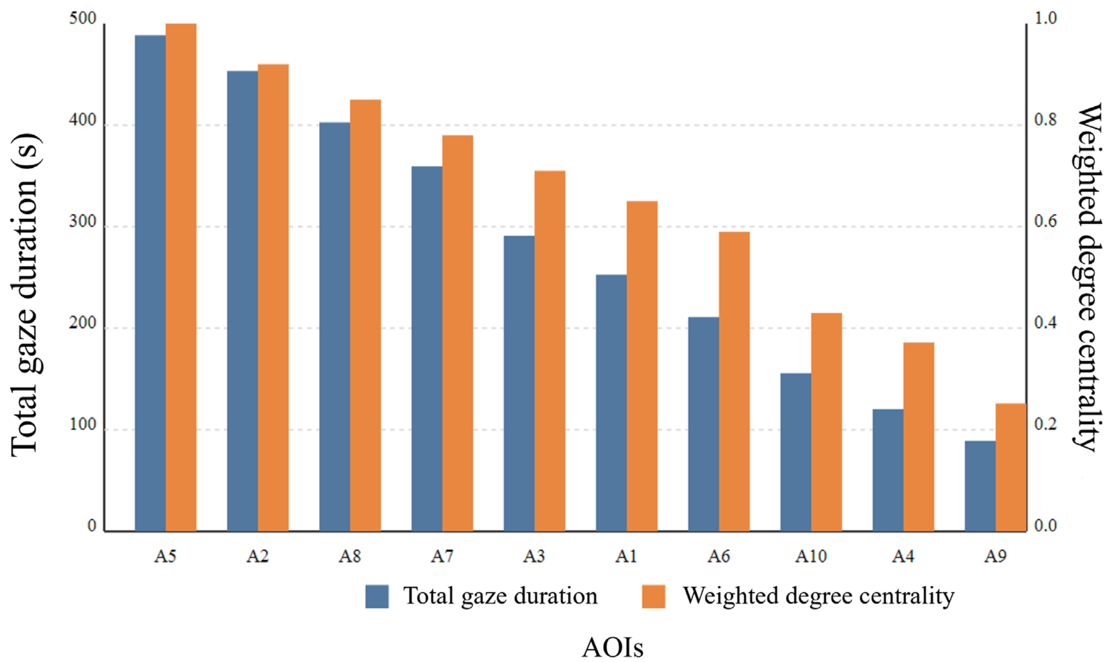

Fig. 4. (Color online) Total gaze duration and weighted degree centrality of AOIs.

sensor-derived gaze metrics effectively capture temporal and structural aspects of user attention. The integration of multimodal sensors allowed for real-time synchronization of pupil diameter and fixation data, enhancing the reliability of attention mapping compared with traditional static AOI analysis.(13)

4.1.2 Mining of high-frequency cognitive paths

Using the transition frequency attribute recorded by the eye-tracking sensors, we identified the most frequent visual transitions between AOIs. The data obtained in the experiment were modeled as a weighted directed graph, where edges represent gaze transitions and nodes represent AOIs. Dijkstra's algorithm was applied to extract high-frequency paths of lengths 2–3, revealing distinct behavioral patterns.(28) Table 8 and Fig. 5 show the top ten single-step

Table 8
High-frequency transition paths (single-step).

Rank	Path	Frequency	Description
1	A2 → A3	289	From main product image to product title
2	A3 → A5	275	From product title to price information
3	A1 → A2	261	From brand logo to main product image
4	A5 → A6	248	From price information to promotional activities
5	A2 → A5	230	Direct transition from main product image to price information
6	A5 → A8	215	From price information to user reviews
7	A8 → A7	198	From user reviews to technical specifications
8	A7 → A8	185	Reciprocal checking between technical specifications and user reviews
9	A3 → A2	179	From product title back to main product image
10	A5 → A10	165	From price information to purchase button

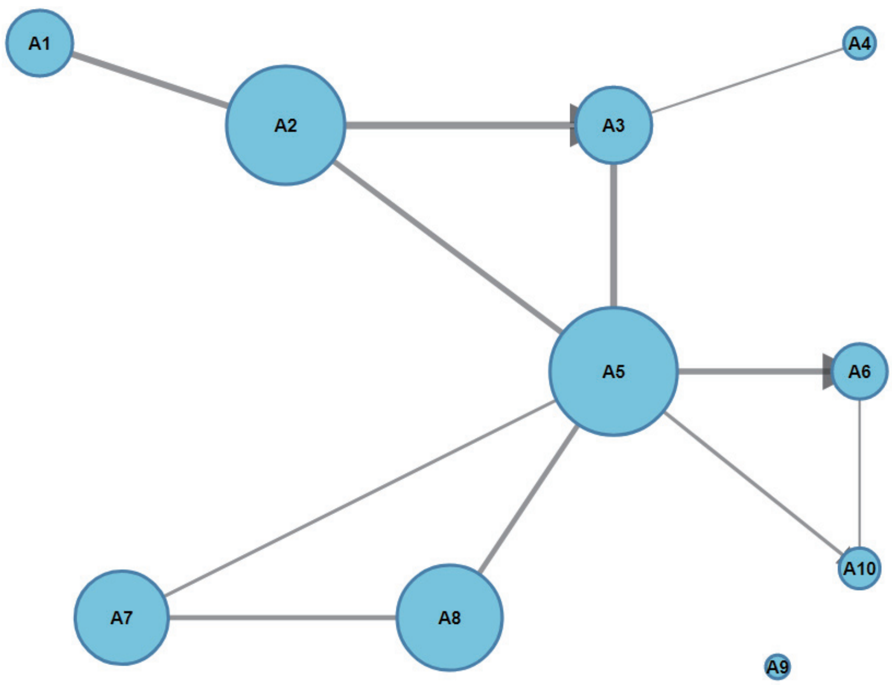

Fig. 5. (Color online) Cognitive path KG (size of circles is proportional to frequency in Table 6).

transitions. The most prominent path—A1 → A2 → A3 → A5—represents the overview-to-valuation sequence, a typical cognitive route for product evaluation. The price–review–specification loop (A5 ↔ A8, A5 ↔ A7) reflects users' cost–benefit reasoning, whereas the impulsive decision path (A5 → A6 → A10) highlights rapid transitions triggered by promotional stimuli. The sensor system's high sampling rate (120 Hz) ensured the precise detection of microsaccades and fixation shifts, enabling the accurate reconstruction of these cognitive pathways. Compared with conventional infrared-based systems,(29) the integrated capacitive sensors demonstrated superior sensitivity to subtle gaze transitions, validating their effectiveness for dynamic path modeling.(2,3)

4.2 Differential analysis based on user groups

Distinct behavioral patterns between new and experienced users were observed in this study. New users exhibited higher path complexity [mean (M) = 1.85, SD = 0.42] than experienced users (M = 1.31, SD = 0.35), indicating more exploratory and repetitive gaze behavior than experienced users. The sensor data captured these differences through variations in fixation dispersion and saccade amplitude, confirming the system's ability to detect nuanced cognitive strategies.(22) New users frequently revisited user reviews (A8) and recommended products (A9), suggesting broader information exploration. In contrast, experienced users followed direct, goal-oriented paths (A1 → A5 and A2 → A10), reflecting efficient decision-making (Table 9, Fig. 6) .

Table 9
Frequency of characteristic paths between new/experienced users.

Path	New user	Experienced user	Significance (significance level)
A8 → A9	45	12	<0.01
A7 → A1	38	8	<0.01
A1 → A5	55	110	<0.001
A2 → A10	25	68	<0.001

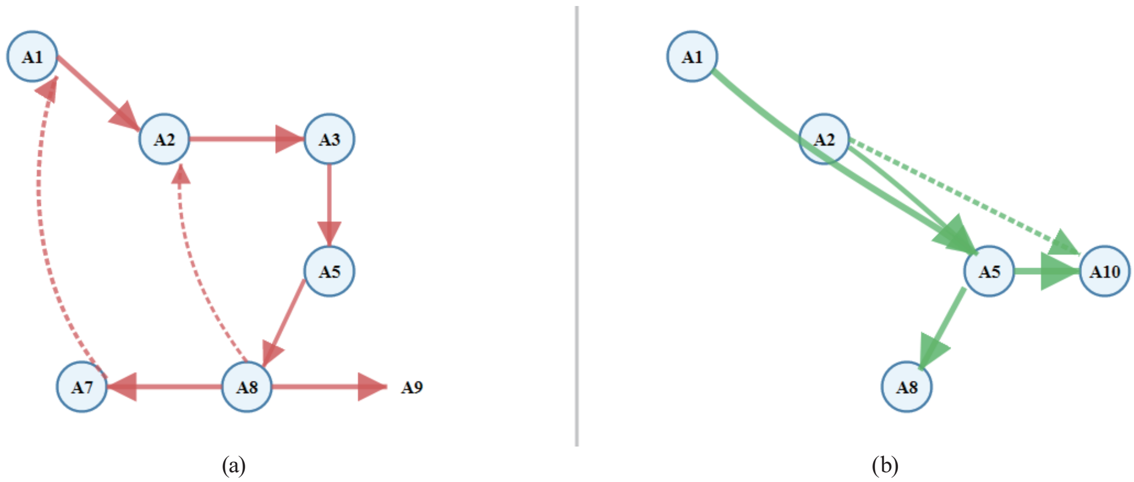

Fig. 6. (Color online) Cognitive path of new and experienced users: (a) New users show more nodes and exploratory paths, and (b) experienced users show fewer nodes and a stronger direct path to key information.

These findings align with prior sensor-based studies on expertise-dependent visual search patterns.[30]

The comparison between impulsive and rational users further demonstrated the sensitivity of the sensor system. Impulsive users exhibited significantly longer fixation durations on promotional activities (A6), whereas rational users focused more on technical specifications (A7) and user reviews (A8). The transition probability from A5 → A6 was 0.45 for impulsive users and 0.21 for rational users, indicating heightened responsiveness to promotional cues (Table 10).

Through the integration of pupil diameter and scanning amplitude data, the physiological validation of the behavioral differences was conducted. Larger pupil dilation and shorter fixation intervals among impulsive users corresponded to higher emotional arousal, consistent with sensor fusion studies on emotion recognition.[12] In contrast, rational users displayed longer fixations and broader scanning ranges, reflecting deliberate information verification. The relationship between path complexity and cognitive load was examined using physiological indicators captured by the eye-tracking sensors: changes in pupil diameter and scanning amplitude. A significant positive correlation was observed ($r = 0.58$, $p < 0.01$), as shown in Fig. 7, indicating that complex browsing paths are associated with increased cognitive effort.[11]

Table 10
Fixation duration on key nodes of impulsive and rational users.

Node	Impulsive users (s)	Rational users (s)	Significance (p-value)
Promotional activities (A6)	4.8	2.2	<0.001
Technical specifications (A7)	4.1	7.8	<0.001
User reviews (A8)	4.5	8.1	<0.001

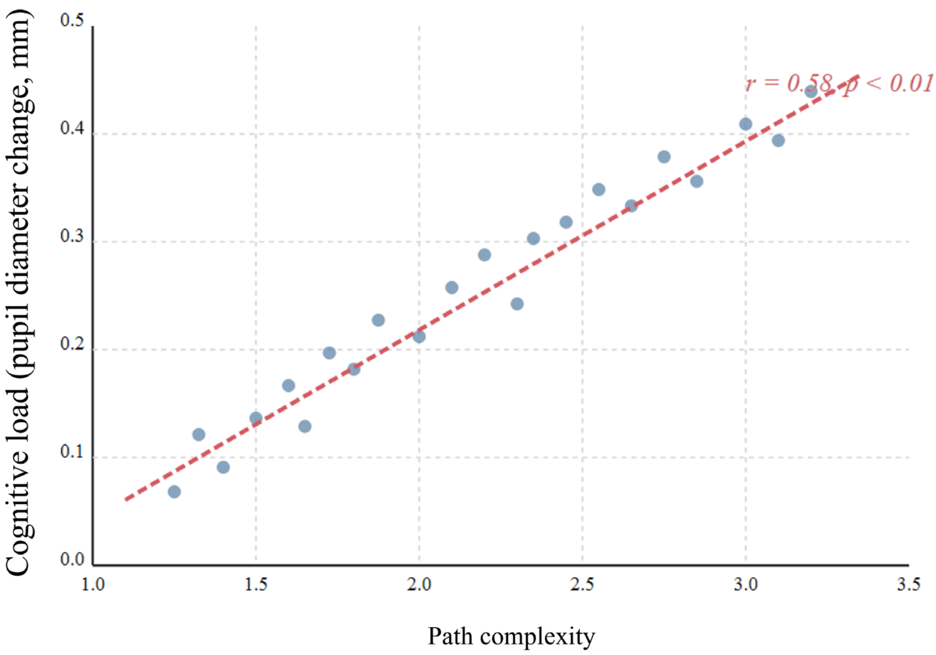

Fig. 7. (Color online) Relationship between path complexity and cognitive load (pupil diameter change).

The result underscores the effectiveness of sensor technology in quantifying cognitive workload. The capacitive and piezoelectric sensors enabled high-resolution pupil tracking, enabling precise measurement of micro-diameter changes in response to visual complexity.(4) The results confirm that sensor-integrated cognitive path modeling can serve as a reliable proxy for mental load assessment, bridging physiological and behavioral data streams. The integration of eye-tracking sensors, graph-based modeling, and KG analytics represents a significant advancement in cognitive behavior research. The system demonstrated high sensitivity, stability, and interpretability across diverse user groups. Combined physiological and behavioral data enable the real-time mapping of cognitive pathways, offering potential applications in neuromorphic vision sensing,(14) human–computer interaction,(23) and emotion-aware marketing systems.(12) Despite the favorable results of this study, sensor modalities must be expanded to include other physiological data, such as electroencephalogram and electrodermal activity, to fuse multimodal sensor data and enhance the granularity of cognitive state detection. Additionally, adaptive algorithms leveraging deep learning need to be integrated to refine transition probability estimation and improve predictive accuracy for user decision-making patterns.

4.3 Limitation and further study

4.3.1 Sensor and modeling constraints

Despite the accuracy of the 250 Hz desktop sensor, two limitations remain. First, the fixed chin-rest setup restricts head movement and natural eye–head coordination, which are essential in unconstrained retail environments. Second, the offline graph construction in Neo4j prevents real-time interface adaptation. To overcome these limitations and enable real-time intent prediction with adaptive interface responses, wearable flexible sensor arrays and graph neural networks (GNNs) must be employed. Wearable flexible sensor arrays provide continuous monitoring of ocular and physiological signals in natural settings without constraining movement.(20,21) Integrated into lightweight glasses or skin-conformal patches, they capture gaze dynamics, pupil dilation, and head orientation during mobile browsing or in-store shopping. This mobility expands data collection beyond static desktop setups, providing ecologically valid insights into consumer behavior. GNNs complement these sensors by processing high-frequency, multimodal data streams in real time.(31) By learning dynamic node and edge representations, GNNs enable adaptive modeling of cognitive pathways as they evolve. Flexible sensor arrays and GNNs establish a responsive framework that bridges physiological sensing with adaptive human–computer interaction, advancing neuromorphic vision and personalized digital marketing.

4.3.2 Information reliability and overload

The objective of the developed framework is to mitigate information overload by filtering redundancy and extracting high-value signals. Its structural design also offers secondary benefits for reducing misleading or erroneous information. The framework naturally down-weights noisy, anomalous, or unverified input streams through the enforcement of strict relevance thresholds and evaluating cross-source consistency during data aggregation. Consequently, low-confidence or contradictory data are suppressed before final representation. However, volume-filtering mechanisms alone cannot fully identify sophisticated or semantically plausible disinformation. Future extensions must integrate automated veracity verification, source-reputation scoring, and cross-modal fact-checking modules into the preprocessing stage.

4.3.3 Demographic generalizability

This study was conducted primarily on young adults, who represent the most active segment of online consumers and are highly familiar with digital marketing environments. Nevertheless, the methodological framework, high-frequency eye-tracking combined with KG modeling, is not limited to this demographic. Older adults exhibit different cognitive pathways, such as longer fixation durations or greater reliance on textual information, but the same sensor-integrated approach can capture and model these behaviors. Extending the method to older populations would support the design of inclusive product pages and adaptive interfaces that accommodate diverse cognitive styles. In this way, the framework enhances personalized marketing for younger users while also improving accessibility and usability across age groups.

4.3.4 Hardware and smart material innovations

In this study, we employed state-of-the-art optoelectronic sensing to construct cognitive KGs. The findings provide specifications for advancing sensor hardware and smart materials. Regarding event-driven CMOS sensor architectures, critical cognitive transitions and visual re-orientations occur within microsaccadic windows (< 20 ms). Current fixed-frame-rate sensors (250 Hz) either miss transient micromovements or generate redundant data during prolonged fixations. These results can inform the development of event-based asynchronous CMOS vision sensors (neuromorphic event-driven sensors) that dynamically adjust sampling rates on the basis of real-time ocular velocity, thereby reducing power consumption in wearable eye-tracking systems.[32] To overcome movement constraints of desktop setups, next-generation sensors fabricated from soft, biocompatible materials must be employed. For high-precision pupil edge detection, wearable systems can integrate high-refractive-index polymer waveguides with flexible organic near-infrared LED matrices, enabling lightweight eyewear that delivers stable illumination without optical distortion.[33] These materials allow natural head and eye coordination while maintaining measurement accuracy.

In addition, closed-loop smart display interfaces can be developed by coupling real-time graph centrality metrics with adaptive materials. Electrochromic polymers and active hydrogel substrates can serve as cognitive-responsive display layers. When ocular metrics such as pupil dilation indicate excessive cognitive workload, these smart materials can dynamically adjust light transmittance, local contrast, or tactile feedback on physical surfaces.[33] Such integration enables adaptive human–computer interfaces that respond directly to physiological signals, advancing neuromorphic vision sensing and personalized digital environments.

5. Conclusion

A robust data-driven method was used for mapping dynamic cognitive pathways by integrating highfrequency eye-tracking sensors with graph-theoretic modeling. By constructing a KG of brand information reading, we verified the initial hypotheses and uncovered deeper insights into user attention, navigation strategies, and cognitive load. The AOI analysis results showed that price information (485.6 s gaze duration, 1.00 normalized weighted degree centrality), product appearance (main product image, 450.2 s), and user reviews (398.1 s) serve as the primary attractors of attention and decision anchors. Graph extraction revealed a dominant overview-to-valuation path (brand logo $\rightarrow$ main product image $\rightarrow$ product title $\rightarrow$ price information) with single-step transitions such as main product image $\rightarrow$ product title (frequency = 289) and product title $\rightarrow$ price information (frequency = 275). Differentiation analysis results showed the potential of sensor-based profiling: new users exhibited significantly higher path complexity (M = 1.85, SD = 0.42) owing to exploratory browsing than experienced users (M = 1.31, SD = 0.35), who utilized goal-oriented shortcuts (brand logo $\rightarrow$ price information frequency = 110 vs 55). Similarly, impulsive users favored promotional cues (price information $\rightarrow$ promotional activities transition probability = 0.45; promotional activities fixation = 4.8 s and 2.2 s), whereas rational users allocated more time to technical parameters (technical specifications, 7.8 s) and user reviews (8.1 s). Correlation analysis confirmed a strong positive relationship between path complexity and pupil-based cognitive load ($r = 0.58$, $p < 0.01$).

The developed framework transforms raw, isolated eye-tracking metrics into dynamic, topological cognitive pathways. By fusing high-precision oculomotor monitoring (250 Hz sampling rate, 0.03° precision), capacitive and piezoelectric sensor components, and multimodal data streams, we obtain a framework that also enables the real-time synchronization of pupil dynamics, microsaccades, and fixation shifts. These advancements provide a physiological foundation for next-generation sensor-integrated human–computer interaction, event-driven neuromorphic vision sensing, and emotion-aware interfaces.

Despite these contributions, limitations remain regarding the physical sensing environment and processing architectures. The reliance on desktop-mounted eye trackers with chin rests constrains natural head–eye movement, limiting ecological validity in unconstrained settings. Furthermore, offline database construction prevents real-time interface adaptation. To overcome these limitations, it is necessary to incorporate wearable flexible sensor arrays, expand participant demographics, and integrate dynamic machine learning models, such as GNNs, to achieve real-time user intent prediction and continuous cognitive state monitoring.

References

1 S. Ban, Y. J. Lee, K. R. Kim, J. Kim, and W. H. Yeo: Biosensors **12** (2022) 11. https://doi.org/10.3390/BIOS12111039
2 X. Jin, C. Gao, X. Zhou, T. Ma, H. Zhao, Z. Zhou, and K. Wang: SID Symp. Dig. Tech. Pap. **55** (2024) 1533. https://doi.org/10.1002/SDTP.17848
3 T. Li, V. Sakthivelpathi, Z. Qian, R. Soetedjo, and J. H. Chung: J. Neurosci. Methods **410** (2024) 110249. https://doi.org/10.1016/J.JNEUMETH.2024.110249
4 N. Kim, J. Chen, W. Wang, J. Kim, M. Kwon, M. Moradnia, and J. Ryou: Adv. Healthc. Mater. **13** (2024) 15. https://doi.org/10.1002/ADHM.202470099

5 P. Lucinskas, M. Deimantavicius, L. Bartusis, R. Zakelis, E. Misiulis, A. Dziugys, and Y. Hamarat: Sci. Rep. **11** (2021) 4736. https://doi.org/10.1038/S41598-021-83777-X
6 L. Drukker, H. Sharma, R. Droste, M. Alsharid, P. Chatelain, J. A. Noble, and A. T. Papageorghiou: Sci. Rep. **11** (2021) 14109. https://doi.org/10.1038/S41598-021-92829-1
7 S. Narasimha, M. Obuseh, N. E. Anton, H. Chen, R. Chakrabarty, D. Stefanidis, and D. Yu: Appl. Ergon. **119** (2024) 104320. https://doi.org/10.1016/j.apergo.2024.104320
8 S. Fuentes, C. Gonzalez Viejo, D. D. Torrico, and F. R. Dunshea: Sensors **21** (2021) 7641. https://doi.org/10.3390/S21227641
9 S. Ma, J. Guo, S. Zeng, H. Che, and X. Pan: Sci. Rep. **12** (2022) 13298. https://doi.org/10.1038/s41598-022-17433-3
10 Y. Li, Y. Gai, X. Wang, L. Sun, and X. Huang: Appl. Sci. **16** (2026) 3580. https://doi.org/10.3390/app16073580
11 F. Kchour, S. Cafiso, and G. Pappalardo: Transp. Res. Part F Psychol. Behav. **119** (2026) 103563. https://doi.org/10.1016/J.TRF.2026.103563
12 M. Kuyucu, M. A. Sarikaya, T. Karakaş, D. Y. Özkan, Y. Demir, Ö. Bilen, and G. Ince: Comput. Biol. Med. **197** (2025) 111070. https://doi.org/10.1016/J.COMPBIOMED.2025.111070
13 T. Li, S. H. Park, C. Lee, S. Kim, Y. Kwon, H. Kim, and J. H. Chung: Adv. Sens. Res. **4** (2025) 7, e00027. https://doi.org/10.1002/ADSR.202500027
14 K. Iddrisu, W. Shariff, M. Stec, N. O'Connor, and S. Little: J. Eye Mov. Res. **19** (2026) 17. https://doi.org/10.3390/JEMR19010017
15 M. Nyström and K. Holmqvist: Behav. Res. Methods **42** (2010) 188. https://doi.org/10.3758/BRM.42.1.188
16 T. Tuntrakool, I. Fongkaew, S. Sangtawesin, J. Widjaja, J. Assawachananont, and P. Meemon: Opt. Continuum **5** (2026) 275. https://doi.org/10.1364/OPTCON.576790
17 Universität Basel: https://psychologie.unibas.ch/fileadmin/user_upload/psychologie/Forschung/N-Lab/SMI_iView_X_Manual.pdf (accseed August 2026).
18 A. Kennedy: Q. J. Exp. Psychol. **69** (2016) 607. https://doi.org/10.1080/17470218.2015.1098709
19 Z. Gomolka, D. Kordos, E. Dudek-Dyduch, and B. Twarog: Appl. Sci. **15** (2025) 11463. https://doi.org/10.3390/app152111463
20 J. Huang, J. Liu, G. Zhang, L. Nie, Y. Xiong, Y. Zhu, Z. L. Wang, and Q. Sun: Nano Energy **150** (2026) 111748. https://doi.org/10.1016/j.nanoen.2026.111748
21 Y. Shi, P. Yang, R. Lei, Z. Liu, X. Dong, X. Tao, X. Chu, Z. L. Wang, and X. Chen: Nat. Commun. **14** (2023) 3315. https://doi.org/10.1038/s41467-023-38987-9
22 J. Tang, P. Luk, and Y. Zhou: Bioeng. **10** (2023) 5. https://doi.org/10.3390/BIOENGINEERING10050514
23 C. Li, Y. Li, X. Liu, S. Xie, Z. Li, Q. Zhou, H.-K Sung, L. Chernogor, Z. Yao, and Y. Li: Adv. Funct. Mater. **36** (2025) e20580. https://doi.org/10.1002/ADFM.202520580
24 G. B. Sproles and E. L. Kendall: J. Consum. Aff. **20** (1986) 267. https://doi.org/10.1111/j.1745-6606.1986.tb00382.x
25 G M. Rajanen and N. Iivari: Lect. Notes Comput. Sci. **4663** (2007) 493. https://doi.org/10.1007/978-3-540-74800-7_47
26 W. P. Bottom: Acad. Manag. Rev. **29** (2004) 695. https://doi.org/10.2307/20159081
27 T. Ryppenthal and N. Schweers: J. Theor. Appl. Electron. Commer. Res. **19** (2024) 1095. https://doi.org/10.3390/jtaer19020057
28 C. Wang, C. Cheng, D. Yang, G. Pan, and F. Zhang: Front. Neurorobot. **16** (2022). https://doi.org/10.3389/fnbot.2022.821991
29 H. Cui, T. Kamijo, M. A. Misran, K. Matsuo, and R. Hattori: SID Symp. Dig. Tech. Pap. **56** (2025) 112. https://doi.org/10.1002/SDTP.18738
30 F. Colonnese, F. Di Luzio, A. Rosato, and M. Panella: Sensors **24** (2024) 7792. https://doi.org/10.3390/S24237792
31 X. Luo, J. Wu, J. Yang, S. Xue, A. Beheshti, and Q. Z. Sheng: Proc. 2024 Int. Joint Conf. Artifical Intelligent (IJCAI, 2024) 8170. https://doi.org/10.24963/ijcai.2024/903
32 P. K. J. Park, J. Kim, J. Ko, and Y. Chang: Electronics **15** (2026) 2828. https://doi.org/10.3390/electronics15132828
33 M. A. Butt: Mater. Today Phys. **64** (2026) 102122. https://doi.org/10.1016/j.mtphys.2026.102122